SInGE: Sparsity via Integrated Gradients Estimation of Neuron Relevance

Edouard Yvinec[1,2] , **Arnaud Dapogny**[2] , **Matthieu Cord**[1] , **Kevin Bailly**[1,2]

Sorbonne Université[1], CNRS, ISIR, f-75005, 4 Place Jussieu 75005 Paris, France

Datakalab[2], 114 boulevard Malesherbes, 75017 Paris, France

`ey@datakalab.com`

Abstract

The leap in performance in state-of-the-art computer vision methods is attributed to the development of deep neural networks. However it often comes at a computational price which may hinder their deployment. To alleviate this limitation, structured pruning is a well known technique which consists in removing channels, neurons or filters, and is commonly applied in order to produce more compact models. In most cases, the computations to remove are selected based on a relative importance criterion. At the same time, the need for explainable predictive models has risen tremendously and motivated the development of robust attribution methods that highlight the relative importance of pixels of an input image or feature map. In this work, we discuss the limitations of existing pruning heuristics, among which magnitude and gradient-based methods. We draw inspiration from attribution methods to design a novel integrated gradient pruning criterion, in which the relevance of each neuron is defined as the integral of the gradient variation on a path towards this neuron removal. Furthermore, we propose an entwined DNN pruning and fine-tuning flowchart to better preserve DNN accuracy while removing parameters. We show through extensive validation on several datasets, architectures as well as pruning scenarios that the proposed method, dubbed SInGE , significantly outperforms existing state-of-the-art DNN pruning methods.

1   Introduction

Deep neural networks (DNNs) are ubiquitous in modern solutions for most computer vision problems such as image classification [1], object detection [2] and semantic segmentation [3]. However, this performance was achieved at the price of high computational requirements and memory foot-print. As such, over-parameterization [4] is a common trait of well performing DNNs that may hinder their deployment on mobile and embedded devices. Furthermore, in the case of deployment on a cloud environment, latency and energy consumption are of paramount importance.

Consequently, compression and acceleration techniques aim at tackling the issue of DNN deployment. Among these methods, pruning approaches consist in removing individual weights (*unstructured* pruning) or entire computational blocks, such as neurons channels or filters (*structured* pruning) [5, 6, 7, 8]. The sparsity induced by pruning reduces both the computational cost and the memory foot-print of neural networks. To do so, there exists a wide variety of heuristics behind such pruning techniques. A few examples are: pruning at initialization [9], grid search [10, 11], magnitude-based [12] or redundancy based [7, 13] approaches. Among such heuristics, magnitude-based pruning remains the favoured one [14, 15, 16]. It consists in defining a metric to assess the relevance of each neuron in the network, with the goal to remove the least important ones while still preserving the predictive function as much as possible. An important limitation of these methods lies in the choice of this importance criterion: magnitude-based criteria [17] do not take into account the whole computations performed in the network (e.g. within the other layers) and gradient-based [18] criteria

are intrinsically local within the neighborhood of a current value or set thereof: from this perspective, setting a value abruptly to zero might break this locality property.

To craft a better criterion, we borrow ideas from the field of DNN attribution [19]. These methods aim at understanding the behavior of a neural network, *i.e.*, in the case of a computer vision model, by providing visual cues of the most relevant regions in a image for the prediction of a network. Tools developed to explain individual predictions are also often called visual explanation techniques [20, 21, 22, 23, 24]. One example of such model is the Integrated Gradient method [24] that consists in defining the contribution of each input by the influence of marginal local changes in the input on the final prediction. This provides a fine-grained evaluation of the importance of each pixel of the image (alternatively, of an intermediate feature map) in the final decision.

Our work is based on the idea that DNN pruning and attribution methods share an important notion, namely that they both rely on the definition of an importance metric to compare several variables of a multidimensional prediction system: for pruning, to remove the least important DNN *parameters*, and, for attribution, to highlight the most important *pixels*. With this in mind, we propose to adapt the integrated gradient method for pruning purposes. Specifically, for each parameter (or set thereof, if we consider structured sparsity), we define its importance as an integral of the product between the norm of this weight and its attribution along a path between this weight value and a baseline (zero) value. By doing so, we avoid pathological cases which less sophisticated gradient-based methods are subjected to such as weights that can be reduced but not zeroed-out without harming the accuracy of the model. Furthermore, we embed the proposed integrated gradient method within a re-training framework to maximize the accuracy of the pruned DNN. We name our method SInGE , standing for **S**parsity *via* **In**tegrated **G**radients **E**stimation of neuron relevance. In short, the contributions of this paper are the following:

- We discuss the limitations of existing pruning heuristics, among which magnitude and gradient based methods. We draw inspiration from attribution methods to design an integrated gradient criterion for estimating the importance of each DNN weight.

- We entwine the updates of the importance measurement within the fine-tuning flowchart to preserve the better DNN accuracy while pruning.

- The proposed approach, dubbed SInGE, achieves superior accuracy *v.s.* pruning ratio on every tested dataset and architecture, compared with recent state-of-the-art approaches.

2   Related Work

2.1   Pruning

Pruning methods are often classified as either structured [25, 26, 27, 10, 28] (filters, channels or neurons are removed) or unstructured [15, 29, 30, 31] (single scalar weight values are set to zero). In practice, the former offers straightforward implementation for inference and immediate runtime benefits but at the price of a lower number of parameters removed. For instance, in GDP [32], weights are pruned with a learned gate that zeroes-out some channels for easier pruning post-training. In CCP [33], sparsity is achieved by evaluating the inter-channel dependency and the joint impact of pruned and preserved channels on the final loss function. In HAP [34], authors replace less sensitive channels based on the trace of the Hessian of predictive function with respect to the weights. Generally speaking, these methods rely on defining a criterion to estimate and compare the importance of weights in the networks, and remove the least important such candidates. A limitation of these methods is that the proposed criteria are usually only relevant within the neighborhood of the current value for a considered weight, which can be problematic since abruptly setting this weight value might violate this locality principle. In this work, we address this limitation by borrowing ideas from the DNN attribution field.

2.2   Attribution

Attribution methods, also referred to as visual explanation methods [20, 21, 22, 23, 24] measure the importance of each input feature on the prediction. Their use was motivated by the need for explainable models [19] as well as constrained learning [35]. We can classify attribution as either occlusion-based or gradient-based. The latter usually offers satisfactory results at a much lower
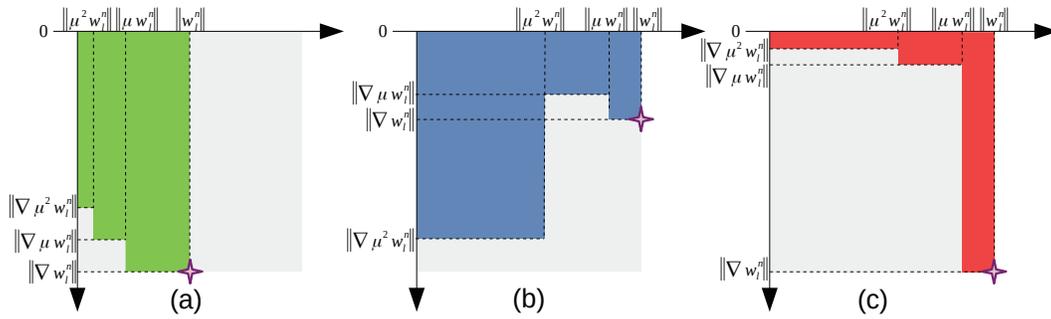
Figure 1: Illustration of possible limitations of traditional pruning criteria for 3 distinct cases and neurons (a,b,c). For a neuron n at layer l we plot the weights norm $||\mu^s w_l^n||$ and corresponding gradients norm $||\nabla \mu^s w_l^n||$ of different neurons (a, b and c) for different powers of $\mu^s \in]0;1[$ corresponding to a path towards zeroing out this neuron. Magnitude-based approaches **(a)** remove low magnitude neurons regardless of the sensitivity (gradient norm) of the predictive function w.r.t. these neurons. Gradient-based approaches **(b)** are limited by the intrinsic locality of the gradient, and abruptly setting a neuron weights to zero may break this locality principle. Conversely, our integrated gradient-based approach **(c)** will prune neuron although it initially has a high magnitude and gradient, integrating its gradient variations along a path down to zero magnitude.

computational cost. Considering that most DNNs for classification are derivable, Grad-CAM [36] computes the gradients of the predictive function with respect to feature maps and weights these gradients by the features. The resulting importance maps are then processed by a ReLU function to extract the features that should be increased in order to increase the value of the target class. Another gradient-based attribution of interest is Integrated-Gradients [24]. In this work, Sundararajan *et al.* propose to sum the gradients of the predictive function with respect to the feature maps over a uniform path in the feature space between feature at hand and a reference point. The resulting attribution maps are usually sharper than maps obtained by Grad-CAM. In the proposed method, we draw inspiration from these methods as we propose to integrate the (local) evolution of the pruning criteria throughout a path going from the current weight value down to a baseline (zero) value. This way, we can smoothly bring the most irrelevant weights down to zero even using intrinsically local criteria such as gradients or gradients per weight norm products.

3   Methodology

Let $F : \mathcal{D} \mapsto \mathbb{R}^{n_o}$ be a feed forward neural network defined over a domain $\mathcal{D} \subset \mathbb{R}^{n_i}$ (e.g. the training dataset in most instances) and an output space $\mathbb{R}^{n_o}$. The operation performed by a layer f_l, for $l \in \{1, \ldots, L\}$, is defined by the corresponding weight tensor $W_l \in \mathcal{A}^{n_{l-1} \times n_l}$ where $\mathcal{A}$ is simply $\mathbb{R}$ in the case of fully-connected layers and $\mathbb{R}^{k \times k}$ in the case of a $k \times k$ convolutional layer. For the sake of simplicity, we assume in what follows that $\mathcal{A} = \mathbb{R}$, *i.e.* we remove neurons as represented by their weight vectors.

3.1   Simple baseline pruning criteria

One major component of pruning methods lies in the definition of an importance measurement for each neuron. The most straightforward such criterion is based on the magnitude of the weight vectors. In such a case, the importance criterion C_{L^p} based on the L^p norm $\| \cdot \|_p$, is defined as:

$$C_{L^p} : (W_l, F, \mathcal{D}) \mapsto (\|W_l^n\|_p)_{n \in \{1, \ldots, n_l\}} \tag{1}$$

where W_l^n is the nth column of W_l, corresponding to the weight values associated with the nth neuron of layer f_l. The transformation C_{L^p} operates layer per layer and independently of the rest of network F and the domain $\mathcal{D}$. Intuitively, C_{L^p} assumes that the least important neurons are the smallest in norm because such neurons have a lower impact on the predictions of F. Such a simple criterion however face limitations: consider for instance the two first neurons (a) and (b) depicted in Figure 1 by the purple stars in two-dimensional spaces as function of their magnitude and gradient norm respectively denoted $\|W_l^n\|$ and $\|\nabla W_l^n\|$, for simplicity. However, we can clearly see how these local measurements provide a wrong evaluation of the cost of pruning these neurons. In such a case,

pruning according to C_{L^p} will remove neuron (a) regardless of the fact that the predictive function F will be very sensitive to small modification of this neuron, as indicated by the large value of its gradients. This is however not the case with the gradient-based pruning criterion C_{∇^p} defined as:

$$C_{\nabla^p} : (W_l, F, \mathcal{D}) \mapsto \left(\left\| \nabla_{W_l^n} F(\mathcal{X} \in \mathcal{D}) \right\|_p \right)_{n \in \{1, \ldots, n_l\}} \tag{2}$$

where $\nabla_{W_l^n} F(\mathcal{X} \in \mathcal{D})$ is the gradient of F with respect to W_l, evaluated on $\mathcal{X}$ a sample from $\mathcal{D}$. Intuitively, the latter measurement puts more emphasis on neurons that can be modified without directly altering the predictive function F. However, a neuron may have a low gradient norm and still strongly contribute to the predictive function, e.g. in the case where the weight is large as in the case of neuron (b) on Figure 1. To handle this, the norm $\times$ gradient criterion $C_{L^p \times \nabla^p}$ straightforwardly combines the best of both worlds:

$$C_{L^p \times \nabla^p} : (W_l, F, \mathcal{D}) \mapsto \left(\left\| W_l^n \right\|_p \times \left\| \nabla_{W_l^n} F(\mathcal{X} \in \mathcal{D}) \right\|_p \right)_{n \in \{1, \ldots, n_l\}} \tag{3}$$

3.2 Integrating gradients towards neuron removal

The importance criterion $C_{L^p \times \nabla^p}$ in Equation (3) faces another kind of limitation. due to the local nature of gradient information: if we consider neuron (b) on Figure 1, this neuron may initially (*i.e.* within a neighborhood of the purple star) have a low gradient norm or even low magnitude per gradient norm product. However, the gradient becomes larger as we bring this value down to 0. This is due to the fact that $\nabla_{W_l^n} F(\mathcal{X} \in \mathcal{D})$ only holds within a neighborhood of W_l^n current value, and abruptly setting this neuron weights to zero may very well violate this locality principle. Thus, inspired from attribution methods, we propose a more global integrated gradient criterion. Formally, for neuron n of a layer, l, we define $\mathcal{I}_l^n$ as the following integral:

$$\mathcal{I}_l^n = \int_{\mu=0}^1 \left\| \nabla_{\mu W_l^n} F(\mathcal{X} \in \mathcal{D}) \right\|_p d\mu \tag{4}$$

Intuitively, we measure the cost of progressively decaying the weights of neuron n and integrating the gradient norm throughout. In practice, we approximate $\mathcal{I}_l^n$ with the following Riemann integral:

$$C_{\text{IG}^p} : (W_l, F, \mathcal{D}) \mapsto \left(\sum_{s=0}^S \left\| \mu^s W_l^n \right\|_p \times \left\| \nabla_{\mu^s W_l^n} F(\mathcal{X} \in \mathcal{D}) \right\|_p \right)_{n \in \{1, \ldots, n_l\}} \tag{5}$$

where $\mu \in]0; 1[$ denotes an update rate parameter. C_{IG^p} approximates $(\mathcal{I}_l^n)_{n \in \{1, \ldots, n_l\}}$ up to a multiplicative constant. Practically, this criterion measures the cost (as expressed by its gradients) of progressively bringing W_l^n down to 0 by S successive multiplication with the update rate parameter μ: the higher μ, the more precise the integration at the expanse of increasing number of computations S. Also note that, similarly to Equation 2, we can get rid of the weight magnitude term in Equation 5 to obtain criterion C_{SG^p}, based on the sum of gradient norms. Explicitly, we get $C_{\text{SG}^p} : (W_l, F, \mathcal{D}) \mapsto$ $\left(\sum_{s=0}^S \left\| \nabla_{\mu^s W_l^n} F(\mathcal{X} \in \mathcal{D}) \right\|_p \right)_{n \in \{1, \ldots, n_l\}}$. In the case depicted on Figure 1, we will prune neuron (c) as its gradient quickly diminishes as its magnitude becomes lower, despite high initial values for both magnitude and gradient. Thus, the proposed integrated gradients criterion C_{IG^p} allows to take into account both the magnitude of a neuron's weights and the sensitivity of the predictive function w.r.t. small (local) variations of these weights. Furthermore, it measures the cost of removing this neuron by smoothly decaying it, re-estimating the gradient value at each step, hence preserving the local nature of gradients.

3.3 Entwining neuron pruning and fine-tuning

In order to preserve the accuracy of the network F, we alternate between removing the neurons and fine-tuning the pruned network using classical stochastic optimization updates. More specifically, given ρ a global pruning target for the whole network F, we define layer-wise pruning objectives

$(\rho_l)_{l \in \{1, \ldots, L\}}$ such that $\sum_{l=1}^{L} \rho_l \times \Omega(W_l) = \rho \times \Omega(F)$ where $\Omega(W_l)$ and $\Omega(F)$ denote the number of parameters in W_l and F, respectively. Similarly to [13], we tested several strategies for the per-layer pruning rates and kept their per-block strategy. Then, we sequentially prune each layer, starting from the first one, by first evaluating the relevance of each neuron $(C_{\text{IG}^p}(W_l, F, \mathcal{D}))_{n \in \{1, \ldots, n_l\}}$ (with parameter μ) in layer l. We then rank the neurons by ascending numbers of importance and select the first, least important one. Notice at this point that if we remove neuron n we have to recompute the criterion C_{IG^p} for all other neurons: in fact, during the first pass, the gradients $\nabla_{\mu^s W_l^n} F(\mathcal{X} \in \mathcal{D})$ were computed with $W_l^n \neq 0$ and are bound to be altered with the removal of neuron n, thus affecting the order of the $n_l - 1$ remaining neuron importance. Last but not least, once layer l is pruned, we perform O finetuning steps (which corresponds to O gradient descent optimization steps) to retain the network accuracy. This method, dubbed SInGE for **S**parsity *via* **In**tegrated **G**radients **E**stimation of neuron importance, is summarized in Algorithm 1.

Algorithm 1 SInGE Algorithm

Require: neural network F, hyper-parameters : O, μ and $(\rho_l)_{l \in \{1, \ldots, L\}}$ and dataset $\mathcal{D}$
  for $l \in \{1, \ldots, L\}$ **do**
    while pruning_rate$(W_l) \leq \rho_l$ **do**   ▷ wait until we reach the goal
        evaluate $M \leftarrow C_{\text{IG}^p}(W_l, F, \mathcal{D})$ ▷ magnitude estimation
        find $n = \arg\min\{M\}$ ▷ find the neuron to prune
        set $W_l^n \leftarrow 0$ ▷ the pruning is performed here
        for $o \in \{1, \ldots, O\}$ **do**
            finetune the whole network F over a batch from $\mathcal{D}$
        end for
    end while
  end for

Empirically, as we show through a variety of experiments that the proposed integrated gradients-based neuron pruning, along with efficient entwined fine-tuning allows to achieve superior accuracy *vs.* pruning rate trade-offs, as compared to existing methods.

4 Experiments

First, we introduce our experimental setup, including the datasets and architectures as well as the implementation details to ensure reproducibility of the results. Second, we validate our approach on Cifar10 dataset by showing the interest of the proposed integrated gradient criterion, as well as the entwined pruning and fine-tuning scheme. We also compare our results with existing approaches on Cifar10. Last but not least, we demonstrate the superior performance of our SInGE method on several architectures on ImageNet compared with state-of-the-art approaches for both structured and unstructured pruning.

4.1 Experimental setup

Datasets and Architectures: we evaluate our models on the two *de facto* standard datasets for architecture compression, *i.e.* Cifar10 [37] and ImageNet [38]. We use the standard evaluation metrics for pruning, *i.e.* the % of removed parameters as well as the % of removed Floating-point operations (FLOPs). We apply our approach on ResNet 56 ([1] with 852K parameters and accuracies 93.46%) on Cifar10 and ResNet 50 ([1] with 25M parameters and 76.17 accuracy on ImageNet), as well as MobileNet v2 [39] backbone on ImageNet with 71.80 accuracy and 3.4M parameters.

Implementation Details: our implementations are based on tensorflow and numpy python libraries. We measured the different pruning criteria using random batches $\mathcal{X}$ of 64 training images for both Cifar10 and ImageNet and fine-tuned the pruned models with batches of size 128 and 64 for Cifar10 and ImageNet, respectively. The number of optimization steps varies from $1k$ to $5k$ on Cifar10 and from $5k$ to $50k$ on ImageNet, while the original models were trained with batches of size 128 and stochastic gradient descent of $78k$ and $2m$ steps on Cifar10 and ImageNet, respectively. All experiments were performed on NVidia V100 GPU. We evaluate our approach both for structured and unstructured pruning: for the former, we use $\mu = 0.9$ and $\mu = 0.95$ for ImageNet and Cifar10,
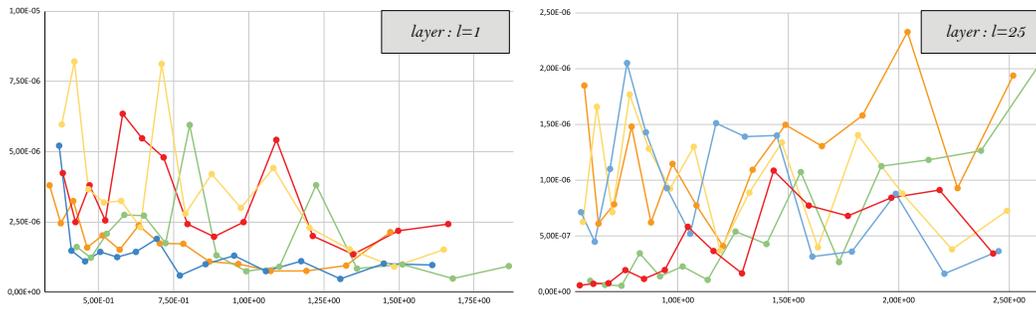
Figure 2: Visualization, for 5 random neurons and two different layers of a ResNet 56 trained on Cifar10, of the evolution of $\left\|\nabla_{\mu^s W_l^n} F(\mathcal{X} \in \mathcal{D})\right\|_p$ (y axis) as the magnitude $\|\mu^s W_l^n\|_p$ (x axis) is brought to 0.

Table 1: Pruning and accuracy performance of the different pruning criterion on a ResNet 56 trained on Cifar10. without fine-tuning. We also report the standard deviation over multiple runs.

Pruning target (% FLOPS / parameters)	pruning criterion	top-1 accuracy
0.0 / 0.0	baseline	93.46
73.03 / 75.00	magnitude C_{L^1}	42.01 ± 0.41
	magnitude C_{L^2}	42.35 ± 0.38
	gradients C_{∇^2}	77.68 ± 0.52
	magnitude $\times$ grad $C_{L^2 \times \nabla^2}$	92.36 ± 0.17
	integrated gradients C_{SG^2}	93.01 ± 0.07
	integrated magnitude $\times$ grad C_{IG^2}	$\mathbf{93.23} \pm 0.23$
86.46 / 85.00	magnitude C_{L^1}	19.14 ± 0.82
	magnitude C_{L^2}	19.13 ± 0.09
	gradients C_{∇^2}	28.31 ± 1.75
	magnitude $\times$ grad $C_{L^2 \times \nabla^2}$	90.28 ± 0.18
	integrated gradients C_{SG^2}	91.90 ± 0.15
	integrated magnitude $\times$ grad C_{IG^2}	$\mathbf{92.80} \pm 0.30$
88.10 / 90.00	magnitude C_{L^1}	$10.00 \pm 1<$
	magnitude C_{L^2}	$10.00 \pm 1<$
	gradients C_{∇^2}	$10.00 \pm 1<$
	magnitude $\times$ grad $C_{L^2 \times \nabla^2}$	$10.00 \pm 1<$
	integrated gradients C_{SG^2}	75.38 ± 1.28
	integrated magnitude $\times$ grad C_{IG^2}	$\mathbf{84.54} \pm 0.91$

respectively. For unstructured pruning, we use $\mu = 0.8$ for ImageNet. In all experiments we performed batch-normalization folding from [40] and measured the pruning ratio using the same metric as SOSP [41].

4.2 Empirical Validation

Pruning Criterion Validation: In Figure 2, we illustrate the evolution of $\left\|\nabla_{\mu^s W_l^n} F(\mathcal{X} \in \mathcal{D})\right\|_p$ (y axis) as the magnitude $\|\mu^s W_l^n\|_p$ (x axis) is brought to 0. This observation confirms the limitations of gradient-based criteria pinpointed in Section 3.2: as the neuron magnitude is progressively decayed, the gradient norm (e.g. yellow curves on both plots, as well as red on the left and blue one on the right plot) for these neurons rise significantly, making these neurons bad choices for removal despite low initial gradient values. This empirical observation suggests that intuition behind the proposed criterion C_{IG^p} is valid. Table 1 draws a comparison between the different criteria introduced in Section 3, applied to prune a ResNet 56 on Cifar10. More specifically, given a percentage of removed operations (or equivalently, percentage of removed parameters), we compare the resulting accuracy

Table 2: Comparison between post-pruning and entwined pruning and fine-tuning on a ResNet 56 on Cifar10.

% Pruning target (% FLOPS / parameters)	fine-tuning	# steps	top-1 accuracy
	post-pruning	1000	92.59
	entwined	1000	**93.18**
86.46 / 85.00	post-pruning	2000	92.66
	entwined	2000	**93.25**
	post-pruning	5000	93.13
	entwined	5000	**93.31**
	post-pruning	1000	77.2
	entwined	1000	**85.38**
88.10 / 90.00	post-pruning	2000	80.89
	entwined	2000	**87.52**
	post-pruning	5000	86.39
	entwined	5000	**90.02**

without fine-tuning. We observe similar trends for the 3 pruning targets: First, using euclidean norm performs slightly better than L_1: thus, we set $p = 2$ in what follows. Second, using gradient instead of magnitude-based criterion allows to significantly improve the accuracy given a pruning target. Third, the magnitude $\times$ gradient criterion $C_{L^2 \times \nabla^2}$ allows to better preserve the accuracy by combining the best of both worlds: for instance, with 85% parameters removed, applying $C_{L^2 \times \nabla^2}$ increases the accuracy by 51.97 points compared with C_{∇^2}. However, those simple criteria face limitations particularly in the high pruning rate regime (90% parameters removed), where the accuracy of the pruned network falls to chance level. Conversely, the proposed integrated gradient-based criteria C_{SG^2} and, *a fortiori* C_{IG^2} allows to preserve high accuracies in such a case. Overall, C_{IG^2} is the best criterion, allowing to preserve near full accuracy with both 85% and 85% removed parameters, and 85.38% accuracy with 90% removed parameters, outperforming the second best method by 8.18 points. For this reason, we will use this criterion (C_{IG^2}) in the following experiments. As the pruning rate increases, the cost of removing a neuron increases and any ill-advised selection of neuron to remove has a growing impact on the accuracy. Consequently, the standard deviation increases as the pruning rate increases this is due to the network expressivity going down.

Fine-tuning Protocol Validation: Table 2 validates our entwined pruning and fine-tuning approach with different pruning targets and number of fine-tuning steps. Specifically, for a given total number of fine-tuning step, we either perform all these steps at once *post-pruning* or alternatively spread them evenly after pruning each layer in an entwined fashion, as described in Section 3.3. First, we observe that simply increasing the number of fine-tuning steps vastly improves the accuracy of the pruned model, particularly in the high % removed parameters regime. Moreover, entwining pruning and fine-tuning performs consistently better than fine tuning after pruning. This suggests that recovering the accuracy is an easier task when performed frequently over small modifications rather than once over a significant modification.

Comparison with state-of-the-art approaches on Cifar10: our approach relies on removing the least important neurons, as indicated by criterion C_{IG^2}. We compare with similar recent approaches such as LP [42] and DPF [29] as well as other heuristics such as training neural networks in order to separate neurons for easier pruning post-training (HAP [34], GDP [32]) or similarity removal (RED [13] or LDI [31]). We report the results in Table 3 for two accuracy set-ups: lossless pruning (accuracy identical to the baseline model) and lossy pruning (≈ 2 points of accuracy drop). The proposed SInGE method significantly outperforms other existing methods by achieving 1.3% higher pruning rate in the lossy setup and a considerable 8.1% improvement in lossless pruning rate. As such, it bridges the gap with unstructured methods such as LP [42] and DPF [29]. This demonstrates the quality of the proposed method.

Table 3: State-of-the-art pruning methods performance on ResNet 56 on Cifar10.

top1 accuracy	pruning method	structured	% parameters removed
	RED [13]	✓	85.0
	LP [42]	✓	84.0
	LP [42]	✗	92.6
91.5 ± 0.1	LDI [31]	✓	88
	DPF [29]	✗	90.0
	HAP [34]	✓	90.0
	SInGE (ours)	✓	$\mathbf{91.3} \pm 0.27$
	GDP [32]	✓	65.6
93.5 ± 0.1	HAP [34]	✓	76.2
	SInGE (ours)	✓	$\mathbf{84.3} \pm 0.71$

Table 4: Comparison between existing structured pruning performance on ResNet 50 on ImageNet. In both the low ($< 50\%$ parameters removed) and high ($> 50\%$) pruning regimes, SInGE achieves remarkable results.

Method	% params rm	% FLOPS rm	accuracy
baseline	0.00	0.00	76.15
Hrank (CVPR 2020) [48]	36.67	43.77	74.98
RED (NeurIPS 2021) [13]	39.6	42.7	76.1
HAP (WACV 2022) [34]	44.59	33.82	75.12
SRR-GR (CVPR 2021) [28]	-	45	75.76
SOSP (ICLR 2021) [41]	49	45	75.21
SRR-GR (CVPR 2021) [28]	-	55	75.11
SInGE	$\mathbf{50.80} \pm 0.02$	$\mathbf{57.35} \pm 0.11$	$\mathbf{76.05} \pm 0.07$
RED (NeurIPS 2021) [13]	54.7	55.0	71.1
SOSP (ICLR 2021) [41]	54	51	74.4
GDP (ICCV 2021) [32]	-	55	73.6
HAP (WACV 2022) [34]	$\mathbf{65.26}$	59.56	74.0
OTO (NeurIPS 2021) [43]	64.1	65.2	73.3
GFP (ICML 2021) [49]	-	65.0	73.94
SInGE	63.78 ± 0.01	$\mathbf{65.96} \pm 0.21$	$\mathbf{74.7} \pm 0.31$

4.3 Performance on ImageNet

Structured Pruning: Table 4 summarizes results obtained by current state-of-the-art approaches in structured pruning. For clarity we divided these results in the low ($<50\%$ parameters removed, where the methods are often lossless) and high pruning regime ($>50\%$ parameters removed with significant accuracy loss). In the low pruning regime, the proposed SInGE method manages to remove slightly more than 50% parameters (57.35% FLOPS) with nearly no accuracy loss, which significantly improves over existing approaches. Second, in the high pruning regime, other methods such as OTO [43] and HAP [34] recently improved the pruning rates by more than 10 points over other techniques such as GDP [32] and SOSP [41]. Nonetheless, SInGE is competitive with these methods and achieve a higher FLOP reduction while maintaining a higher accuracy.

We also evaluated the proposed method on the more compact (thus generally harder to prune) MobileNet V2 architecture. Results and comparison with existing approaches are shown in Table 5. We consider three pruning goals of $\approx 30\%$, $\approx 40\%$ and $\approx 50\%$ parameters removed. First, with near lossless pruning, we achieve results that are comparable to ManiDP-A [44] and Adapt-DCP [45] with a marginal improvement in accuracy. Second, when targeting 40% parameters removed we improve by 0.89% the accuracy with 2.25% less parameters removed as compared to MDP [46]. Finally, in the higher pruning rates, we improve by 0.25% the accuracy with marginally more parameters pruned than Accs [47].

Table 5: Comparison with existing structured pruning methods on MobileNet V2 backbone for ImageNet.

goal	Method	% params rm	% FLOPS rm	accuracy
-	baseline	0.00	0.00	71.80
30%	CBS (arxiv 2022) [50]	30.00	-	71.48
	Adapt-DCP (TPAMI 2021) [45]	**35.01**	30.67	71.4
	ManiDP-A (CVPR 2021) [44]	-	**37.2**	71.6
	SInGE	30.96	31.54	**71.67** $\pm$ 0.06
40%	CBS (arxiv 2022) [50]	40.00	-	69.37
	MDP (CVPR 2020) [46]	**43.15**	-	69.58
	SInGE	40.90	42.30	**70.47** $\pm$ 0.09
50%	CBS (arxiv 2022) [50]	50.00	-	62.96
	Adapt-DCP (TPAMI 2021)	-	45.0	64.13
	ManiDP-A (CVPR 2021)	-	48.8	69.62
	Accs (arxiv 2021) [47]	50.00	-	69.76
	GFP (ICML 2021) [49]	-	50.0	69.16
	SInGE	**50.13**	**48.90**	**70.01** $\pm$ 0.22

Table 6: Comparison with existing unstructured pruning techniques on ResNet 50 on ImageNet.

Method	% params rm	% FLOPS rm	top1 accuracy
DS (NeurIPS 2021) [51]	80.47	72.13	76.15
GMP (arxiv 2019) [52]	80.08	-	76.15
STR (ICML 2020) [53]	79.69	81.17	76.00
RigL (ICML 2020) [54]	80.08	58.92	75.00
SInGE	80.00	82.21	75.12
SInGE	90.00	86.96	73.77

Unstructured Pruning: While being harder to leverage, unstructured pruning usually enables significantly higher pruning rates. Table 6 lists several state-of-the-art pruning methods evaluated on ResNet 50. We observe a common threshold in performance around 80% parameters and FLOPs removed among state-of-the-art techniques. However, the proposed SInGE method manages to achieve very good accuracy of 73.77% while breaking the barrier of pruning performance at 90% parameters removed and almost 87% FLOPs removed. These results in addition to the previous excellent results obtained on structured pruning confirm the versatility of the proposed criterion and method for both structured and unstructured pruning.

5 Conclusion

In this paper, we pinpointed some limitations of some classical pruning criteria for assessing neuron importance prior to removing them. In particular, we showed that magnitude-based approaches did not consider the sensitivity of the predictive function w.r.t. this neuron weights, and that gradient-based approaches were limited to the locality of the measurements. We drew inspiration on recent DNN attribution techniques to design a novel integrated gradients criterion, that consists in measuring the integral of the gradient variation on a path towards removing each individual neuron. Furthermore, we proposed to entwine this criterion within the fine-tuning steps. We showed through extensive validation that the proposed method, dubbed SInGE, achieved superior accuracy *v.s.* pruning ratio as compared with existing approaches on a variety of benchmarks, including several datasets, architectures, and pruning scenarios.

Future work will involve introducing stochasticity in the model weights, similarly to [55], in order to smooth the decision function and ultimately the neuron relevance criterion. Lasty, we will combine our approach with existing similarity-based pruning methods as well as with other DNN acceleration techniques, e.g. tensor decomposition or quantization techniques.

Acknowledgments

References

[1] Kaiming He, Xiangyu Zhang, et al. Deep residual learning for image recognition. *CVPR*, pages 770–778, 2016.

[2] Ross Girshick. Fast r-cnn. *ICCV*, pages 1440–1448, 2015.

[3] Liang-Chieh Chen et al. Deeplab: Semantic image segmentation with deep convolutional nets, atrous convolution, and fully connected crfs. *TPAMI*, pages 834–848, 2017.

[4] Chiyuan Zhang, Samy Bengio, Moritz Hardt, Benjamin Recht, and Oriol Vinyals. Understanding deep learning (still) requires rethinking generalization. *Communications of the ACM*, 64(3):107–115, 2021.

[5] Yann LeCun, John Denker, and Sara Solla. Optimal brain damage. *NeurIPS*, 2, 1989.

[6] Babak Hassibi and David Stork. Second order derivatives for network pruning: Optimal brain surgeon. *NeurIPS*, 5, 1992.

[7] Suraj Srinivas and R Venkatesh Babu. Data-free parameter pruning for deep neural networks. *BMVC*, 2015.

[8] Song Han, Huizi Mao, and William J Dally. Deep compression: Compressing deep neural networks with pruning, trained quantization and huffman coding. *ICLR*, 2016.

[9] Huan Wang, Can Qin, Yulun Zhang, and Yun Fu. Emerging paradigms of neural network pruning. *arXiv preprint arXiv:2103.06460*, 2021.

[10] Jian-Hao Luo, Jianxin Wu, and Weiyao Lin. Thinet: A filter level pruning method for deep neural network compression. *ICCV*, pages 5058–5066, 2017.

[11] Ruichi Yu, Ang Li, Chun-Fu Chen, Jui-Hsin Lai, Vlad I Morariu, Xintong Han, Mingfei Gao, Ching-Yung Lin, and Larry S Davis. Nisp: Pruning networks using neuron importance score propagation. *CVPR*, pages 9194–9203, 2018.

[12] Pavlo Molchanov, Stephen Tyree, Tero Karras, Timo Aila, and Jan Kautz. Pruning convolutional neural networks for resource efficient inference. *arXiv preprint arXiv:1611.06440*, 2016.

[13] Edouard Yvinec, Arnaud Dapogny, Matthieu Cord, and Kevin Bailly. Red: Looking for redundancies for data-freestructured compression of deep neural networks. *Advances in Neural Information Processing Systems*, 34, 2021.

[14] Kun Han, Yuxuan Wang, DeLiang Wang, William S Woods, Ivo Merks, and Tao Zhang. Learning spectral mapping for speech dereverberation and denoising. *IEEE/ACM Transactions on Audio, Speech, and Language Processing*, 23(6):982–992, 2015.

[15] Jonathan Frankle and Michael Carbin. The lottery ticket hypothesis: Finding sparse, trainable neural networks. *ICLR*, 2018.

[16] Pavlo Molchanov, Arun Mallya, Stephen Tyree, Iuri Frosio, and Jan Kautz. Importance estimation for neural network pruning. *CVPR*, pages 11264–11272, 2019.

[17] Guiying Li, Chao Qian, Chunhui Jiang, Xiaofen Lu, and Ke Tang. Optimization based layer-wise magnitude-based pruning for dnn compression. In *IJCAI*, pages 2383–2389, 2018.

[18] Congcong Liu and Huaming Wu. Channel pruning based on mean gradient for accelerating convolutional neural networks. *Signal Processing*, 156:84–91, 2019.

[19] Wojciech Samek, Thomas Wiegand, and Klaus-Robert Müller. Explainable artificial intelligence: Understanding, visualizing and interpreting deep learning models. *arXiv preprint arXiv:1708.08296*, 2017.

[20] David Baehrens, Timon Schroeter, Stefan Harmeling, Motoaki Kawanabe, Katja Hansen, and Klaus-Robert Müller. How to explain individual classification decisions. *JMLR*, 11:1803–1831, 2010.

[21] Karen Simonyan, Andrea Vedaldi, and Andrew Zisserman. Deep inside convolutional networks: Visualising image classification models and saliency maps. *arXiv preprint arXiv:1312.6034*, 2013.

[22] Wojciech Samek, Alexander Binder, Grégoire Montavon, Sebastian Lapuschkin, and Klaus-Robert Müller. Evaluating the visualization of what a deep neural network has learned. *IEEE transactions on neural networks and learning systems*, 28(11):2660–2673, 2016.

[23] Avanti Shrikumar, Peyton Greenside, and Anshul Kundaje. Learning important features through propagating activation differences. *ICML*, pages 3145–3153, 2017.

[24] Mukund Sundararajan, Ankur Taly, and Qiqi Yan. Axiomatic attribution for deep networks. *ICML*, pages 3319–3328, 2017.

[25] Lucas Liebenwein, Cenk Baykal, et al. Provable filter pruning for efficient neural networks. *ICLR*, 2020.

[26] Hao Li et al. Pruning filters for efficient convnets. *ICLR*, 2017.

[27] Yang He, Guoliang Kang, et al. Soft filter pruning for accelerating deep convolutional neural networks. *IJCAI*, pages 2234–2240, 2018.

[28] Zi Wang, Chengcheng Li, and Xiangyang Wang. Convolutional neural network pruning with structural redundancy reduction. *CVPR*, pages 14913–14922, 2021.

[29] Tao Lin, Sebastian U Stich, et al. Dynamic model pruning with feedback. *ICLR*, 2020.

[30] Sejun Park, Jaeho Lee, et al. Lookahead: a far-sighted alternative of magnitude-based pruning. *ICLR*, 2020.

[31] Namhoon Lee, Thalaiyasingam Ajanthan, et al. A signal propagation perspective for pruning neural networks at initialization. *ICLR*, 2020.

[32] Yi Guo, Huan Yuan, Jianchao Tan, Zhangyang Wang, Sen Yang, and Ji Liu. Gdp: Stabilized neural network pruning via gates with differentiable polarization. *ICCV*, pages 5239–5250, 2021.

[33] Hanyu Peng, Jiaxiang Wu, Shifeng Chen, and Junzhou Huang. Collaborative channel pruning for deep networks. *ICML*, pages 5113–5122, 2019.

[34] Shixing Yu, Zhewei Yao, Amir Gholami, Zhen Dong, Sehoon Kim, Michael W Mahoney, and Kurt Keutzer. Hessian-aware pruning and optimal neural implant. *WACV*, pages 3880–3891, 2022.

[35] Jules Bonnard, Arnaud Dapogny, Ferdinand Dhombres, and Kévin Bailly. Privileged attribution constrained deep networks for facial expression recognition. *arXiv preprint arXiv:2203.12905*, 2022.

[36] Ramprasaath R Selvaraju, Michael Cogswell, Abhishek Das, Ramakrishna Vedantam, Devi Parikh, and Dhruv Batra. Grad-cam: Visual explanations from deep networks via gradient-based localization. *ICCV*, pages 618–626, 2017.

[37] Alex Krizhevsky, Geoffrey Hinton, et al. Learning multiple layers of features from tiny images. *Master's thesis, Department of Computer Science, University of Toronto*, 2009.

[38] J. Deng, W. Dong, et al. ImageNet: A Large-Scale Hierarchical Image Database. *CVPR*, 2009.

[39] Mark Sandler, Andrew Howard, et al. Mobilenetv2: Inverted residuals and linear bottlenecks. *CVPR*, pages 4510–4520, 2018.

[40] Edouard Yvinec, Arnaud Dapogny, and Kevin Bailly. To fold or not to fold: a necessary and sufficient condition on batch-normalization layers folding. *IJCAI*, 2022.

[41] Manuel Nonnenmacher, Thomas Pfeil, Ingo Steinwart, and David Reeb. Sosp: Efficiently capturing global correlations by second-order structured pruning. *ICLR*, 2021.

[42] Lucas Liebenwein, Cenk Baykal, Brandon Carter, David Gifford, and Daniela Rus. Lost in pruning: The effects of pruning neural networks beyond test accuracy. *Proceedings of Machine Learning and Systems*, 3:93–138, 2021.

[43] Tianyi Chen, Bo Ji, Tianyu Ding, Biyi Fang, Guanyi Wang, Zhihui Zhu, Luming Liang, Yixin Shi, Sheng Yi, and Xiao Tu. Only train once: A one-shot neural network training and pruning framework. *NeurIPS*, 34, 2021.

[44] Yehui Tang, Yunhe Wang, Yixing Xu, Yiping Deng, Chao Xu, Dacheng Tao, and Chang Xu. Manifold regularized dynamic network pruning. *arXiv preprint arXiv:2103.05861*, 2021.

[45] Jing Liu, Bohan Zhuang, Zhuangwei Zhuang, Yong Guo, Junzhou Huang, Jinhui Zhu, and Mingkui Tan. Discrimination-aware network pruning for deep model compression. *IEEE Transactions on Pattern Analysis and Machine Intelligence*, 2021.

[46] Jinyang Guo, Wanli Ouyang, and Dong Xu. Multi-dimensional pruning: A unified framework for model compression. *CVPR*, pages 1508–1517, 2020.

[47] Asit Mishra, Jorge Albericio Latorre, Jeff Pool, Darko Stosic, Dusan Stosic, Ganesh Venkatesh, Chong Yu, and Paulius Micikevicius. Accelerating sparse deep neural networks. *arXiv preprint arXiv:2104.08378*, 2021.

[48] Mingbao Lin, Rongrong Ji, et al. Hrank: Filter pruning using high-rank feature map. *CVPR*, pages 1529–1538, 2020.

[49] Liyang Liu, Shilong Zhang, Zhanghui Kuang, Aojun Zhou, Jing-Hao Xue, Xinjiang Wang, Yimin Chen, Wenming Yang, Qingmin Liao, and Wayne Zhang. Group fisher pruning for practical network compression. In *ICML*, pages 7021–7032. PMLR, 2021.

[50] Xin Yu, Thiago Serra, Shandian Zhe, and Srikumar Ramalingam. The combinatorial brain surgeon: Pruning weights that cancel one another in neural networks. *arXiv preprint arXiv:2203.04466*, 2022.

[51] Wei Sun, Aojun Zhou, Sander Stuijk, Rob Wijnhoven, Andrew O Nelson, Henk Corporaal, et al. Dominosearch: Find layer-wise fine-grained n: M sparse schemes from dense neural networks. *NeurIPS*, 34, 2021.

[52] Trevor Gale, Erich Elsen, and Sara Hooker. The state of sparsity in deep neural networks. *arXiv preprint arXiv:1902.09574*, 2019.

[53] Aditya Kusupati, Vivek Ramanujan, Raghav Somani, Mitchell Wortsman, Prateek Jain, Sham Kakade, and Ali Farhadi. Soft threshold weight reparameterization for learnable sparsity. In *ICML*, pages 5544–5555. PMLR, 2020.

[54] Utku Evci, Trevor Gale, Jacob Menick, Pablo Samuel Castro, and Erich Elsen. Rigging the lottery: Making all tickets winners. *ICML*, pages 2943–2952, 2020.

[55] Kirill Bykov, Anna Hedström, Shinichi Nakajima, and Marina M-C Höhne. Noisegrad—enhancing explanations by introducing stochasticity to model weights. In *AAAI*, 2022.